

RD-A144 524

THE MANUFACTURING PROCESS AND THE COLD DEPLOYMENT TEST
OF AN EXTENDIBLE N. (U) FOREIGN TECHNOLOGY DIV
WRIGHT-PATTERSON AFB OH H HONG 30 JUL 84

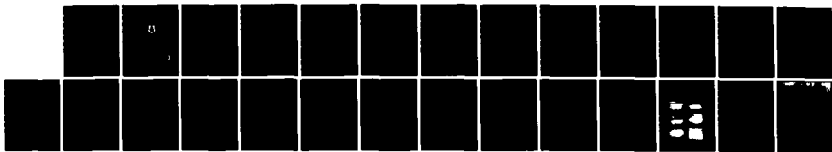
1/1

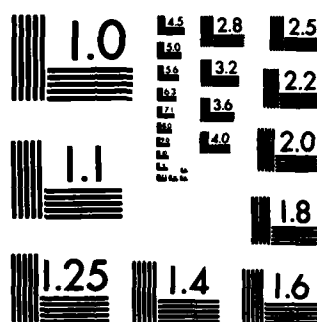
UNCLASSIFIED

FTD-ID(RS)T-0819-84

F/G 11/6

NL





MICROCOPY RESOLUTION TEST CHART
NATIONAL BUREAU OF STANDARDS-1963-A

2

FTD-ID(RS)T-0819-84

FOREIGN TECHNOLOGY DIVISION

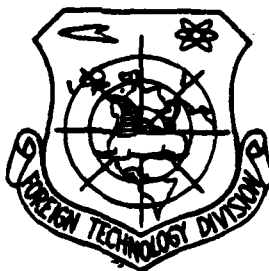
AD-A144 524



THE MANUFACTURING PROCESS AND THE COLD DEPLOYMENT TEST
OF AN EXTENDIBLE NOZZLE MADE OF C-103 NIOBIUM ALLOY

by

Hu Hong



DTIC
ELECTED
AUG 22 1984
S E D

DTIC COPY

Approved for public release;
distribution unlimited.



84 08 21 108

AD-1144-504

FTD-ID(RS)T-0819-84

EDITED TRANSLATION

FTD-ID(RS)T-0819-84

30 July 1984

MICROFICHE NR: FTD-84-C-000752

THE MANUFACTURING PROCESS AND THE COLD DEPLOYMENT
TEST OF AN EXTENDIBLE NOZZLE MADE OF C-103 NIOBIUM
ALLOY

By: Hu Hong

English pages: 22

Source: Yuhang Xuebao, Nr. 4, 1983, pp. 71-80

Country of origin: China

Translated by: LEO KANNER ASSOCIATES
F33657-81-D-0264

Requester: FTD/TQTA

Approved for public release; distribution unlimited.

THIS TRANSLATION IS A RENDITION OF THE ORIGINAL FOREIGN TEXT WITHOUT ANY ANALYTICAL OR EDITORIAL COMMENT. STATEMENTS OR THEORIES ADVOCATED OR IMPLIED ARE THOSE OF THE SOURCE AND DO NOT NECESSARILY REFLECT THE POSITION OR OPINION OF THE FOREIGN TECHNOLOGY DIVISION.

PREPARED BY:

TRANSLATION DIVISION
FOREIGN TECHNOLOGY DIVISION
WP-AFB, OHIO. *45033*

FTD-ID(RS)T-0819-84

Date 30 Jul 1984

GRAPHICS DISCLAIMER

All figures, graphics, tables, equations, etc.
merged into this translation were extracted
from the best quality copy available.

Accession For	
NTIS GRA&I	<input checked="" type="checkbox"/>
DTIC TAB	<input type="checkbox"/>
Unannounced	<input type="checkbox"/>
Justification	
FY	
Distribution/	
Availability Codes	
Avail and/or	
Dist	Special
A-1	



THE MANUFACTURING PROCESS AND THE COLD DEPLOYMENT TEST OF AN EXTENDIBLE NOZZLE MADE OF C-103 NIOBIUM ALLOY

Hu Hong

Abstract

This paper briefly introduces the salient features of the extendible nozzle and the properties of C-103 niobium alloy. Focus of discussion is on the forming technique of this nozzle's medium-sized cold test piece using the shear spinning, extension forming and mandrel diameter expansion processes. We also carried out analytical comparisons of the cold deployment tests of the nozzle and thus provided necessary technical data for the initial sample production of extendible nozzles.

I. Introduction

Use of the extendible nozzle on rocket engines is the adding of an extendible composite section on the diffusion section of the nozzle. It has various forms such as the travelling cup type, folding umbrella type and the apron and contracting types etc. The aim is to cause the engine to contract or fold back the extendible section of the nozzle when in a non-operating state so as to reduce the length of the engine. However, when the engine is ignited, this can rapidly deploy and release the extended section, enlarge the expansion ratio of the nozzle and raise the specific impulse of the engine.

The Bayer Aerospace Company and the United Technology Center of the United States developed the niobium alloy extendible nozzle for the third stage engine of the Trident C₄ missile. The largest exit diameter of the nozzle was $\phi 1397\text{mm}$, the wall thickness was 0.73-1mm, the semi-tapered angle was 19° and the shear spinning technique with no welding seam was used for nozzle forming.

The niobium alloy extendible nozzle introduced in this paper is the folding umbrella type. Development was carried out in three steps. The first step was the small conical nozzle heat test which is designed to investigate the high temperature performance of the niobium alloy; the second step was the medium-sized extendible nozzle cold deployment test which seeks a rational forming technique and investigates the deformation and related parameters of the cold deployment test process; the third step is the formal development of the initial sample of the product.

II. Synopsis of the Performance of the Niobium Alloy and Its Extendible Nozzle

1. Synopsis of the Properties of C-103 Niobium Alloy

Because the extendible nozzle requires expansion and contraction, it is not only necessary that the nozzle material possess certain high temperature strength but it must also have sufficient plasticity. C-103 niobium alloy is an alloy with a high melting point, high plasticity and medium strength. It has excellent high heat endurance properties, formation properties and welding properties and therefore has been widely used in rockets, missiles and the atomic energy industry in recent years.

Table 1 gives the mechanical properties of C-103 plate material. It realizes solid solution strengthening of the alloy by adding Hf, Ti and Zr alloy elements into the niobium. The Zr in the alloy has marked strengthening effects, the Ti can improve the anti-oxidation properties and machining properties of the alloy and Hf and W primarily have high temperature endurance effects in the alloy. Niobium alloy has relatively high solubility towards C, N₂, H₂ and O₂ and forms space impurities. At this time, the influence of the alloy's mechanical properties is relatively large and if there is 0.1% oxygen in the alloy this can cause difficulty in carrying on the cold machining.

When the niobium alloy is above 450°C, the anti-oxidation properties are relatively poor and we should thus give attention to avoiding thermal oxidation during the technological practice. We must use vacuum equipment or inert gas protection for the welding or thermal procedure. Under high temperature conditions, the niobium alloy part used must have an anti-oxidation coating applied on the metallic surface.

(1) 温 度 (3)	屈服强度 σ_{y} , kg/mm ² (4)	抗拉强度 σ_b , kg/mm ² (5)	延伸率 δ % (6)	断面率 ψ % (7)	弹性模量 E kg/mm ² (7)
(2) 室 温	35.5	41~48	26	~70	8800
1482°C	6	5.6	>70		2520

Table 1 Mechanical properties of C-103

Key: (1) Temperature; (2) Room temperature; (3) Yield strength; (4) Tensile strength; (5) Percentage elongation; (6) Percentage section; (7) Elastic modulus.

2. Synopsis of Folding Umbrella Type Extendible Nozzle

The approximate form of the folding umbrella type extendible nozzle's non-operating state is as shown in Fig. 1(a). The instant before the nozzle enters the operating state, the control system operates actuating cylinder 2 which drives extension ring 4 causing the nozzle to extend straight out. Figure 1(b) shows the shape of the nozzle after extending straight out.

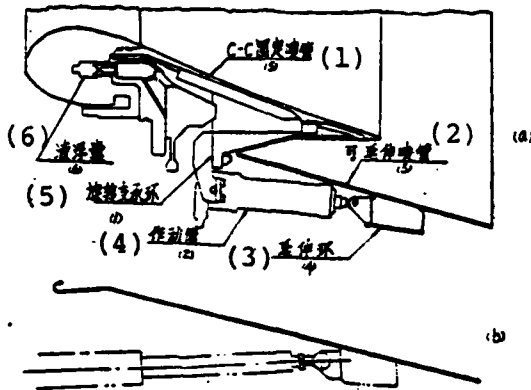


Fig. 1 (a) Assembly condition of extended nozzle; (b) condition after the extended nozzle is deployed.

Key: (1) C-C fixed nozzle; (2) Extendible nozzle;
 (3) Extension ring; (4) Actuating cylinder;
 (5) Rotating support ring; (6) Liquid flotation bag.

The form of the extendible nozzle used for medium-sized cold deployment tests is shown in Fig. 2. The extension ring in the figure is made of titanium alloy and is welded with the nozzle into a whole. The cylinder section in the nozzle has positioning and connecting effects and at the same time participates in extension. The forward and reverse 18° conical wall rotates and connects by the R4 circular arc and this arc is also the initial circular arc of the nozzle's extension deformation. In order to cause the nozzle's conical wall to keep the generating line level and straight after extension, it is necessary to pay attention to maintaining uniformity of each part's wall thickness during the nozzle's forming process. For simplicity and convenience, we first developed plan (a) in Fig. 2 (without a cylinder section) and on the basis of this, then developed plan (b).

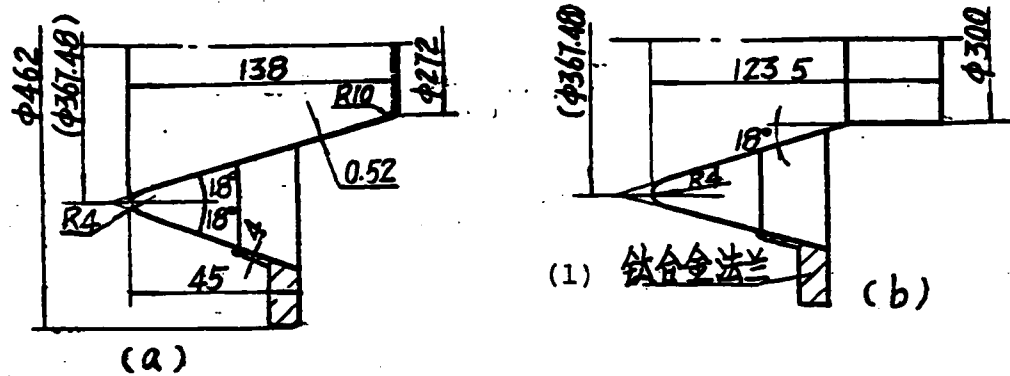


Fig. 2 Plans a and b for medium-sized cold deployed extended nozzle.

Key: (1) Titanium alloy flange.

We took into consideration making the forming assembly simple, having continuity in technology and that use of a strong spinning method for nozzle forming was quite advantageous. However, it was difficult for this method to guarantee uniform wall thickness of the R4 arc and it was therefore necessary to add other supplementary forming techniques which combined with the spinning technique completed the requirements for the forming of the entire nozzle.

III. Forming Process of the Extendible Nozzle

After a series of tests and comparisons, we determined the forming process of the extendible nozzle as shown in Fig. 3.

Each procedure in the forming process of the extendible nozzle used stainless steel 1Cr18Ni9Ti part test moulds so as to economize on the expensive niobium alloy material.

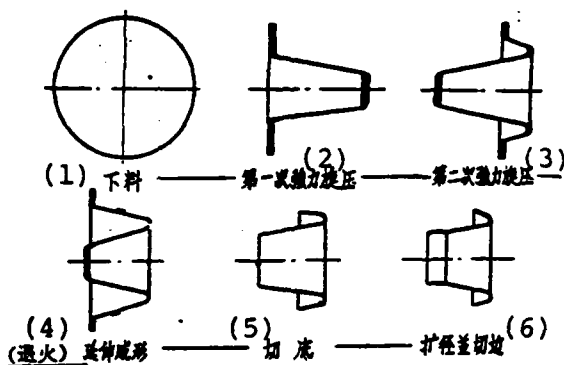


Fig. 3 Forming process of the nozzle.

Key: (1) Lower material; (2) First shear spinning;
 (3) Second shear spinning; (4) (Annealing)
 Extension forming; (5) Sheared base;
 (6) Enlarged diameter and sheared edge.

1. Determination of Spinning Technique

The nozzle's forward and reverse 18° conical wall both use shear spinning forming. The spinning was carried out on a P111B/2 spinning machine and used the single rotating wheel spinning method.

(1) Determination of the Number of Spinning Paths

The number of spinning paths was mainly determined by the plasticity and ultimate thinning rate of the material. The plasticity of C-103 was relatively good and the annealing condition's elongation $\delta \geq 26\%$. The ultimate thinning rate φ_{max} can be approximately calculated based on the section contraction of the material.

If we take the section contraction γ of C-103 as 70%, then its ultimate thinning rate is:

$$\varphi_{max} = \frac{\psi}{0.17 + \psi} \% = \frac{0.7}{0.17 + 0.7} \% = 80\%$$

Further, based on the former experience of the two continuous

shear spinning C-103 plate materials, the slab with a thickness of 3.5mm was spun into a finished product with a thickness of 1.1mm, there was no procedural annealing in the middle and the total thinning rate was:

$$(1) \varphi_s = \frac{t_0 - t}{t_0} \% = \frac{3.5 - 1.1}{3.5} \% = 69\%$$

Key: (1) Total.

It can be determined from this that an extendible nozzle with a semi-tapered angle of 18° can be formed by one spinning and because the thinning rate at this time was:

$$\varphi_s = \left(1 - \sin \frac{\alpha}{2}\right) \% = (1 - 0.3090) \% = 69\%$$

φ_t was smaller than the calculated ultimate thinning rate φ_{max} and was equal to the formerly actually used φ_{total} .

The plasticity of stainless steel was better than that of niobium alloy ($\delta \geq 42\%$) and therefore we can completely spin a part with an 18° semi-tapered angle in one time.

(2) Determination of the Dimensions of the Spinning Slab

The slab thickness of shear spinning was determined based on the law of sines, that is:

$$t = t_0 \sin \frac{\alpha}{2} \quad (1)$$

In the formula

t is the part's thickness (0.8mm);
 t_0 is the slab's thickness;
 $\frac{\alpha}{2}$ is the part's semi-tapered angle (18°);

$$\therefore t_0 = \frac{t}{\sin \frac{\alpha}{2}} = \frac{0.8}{0.3090} = 2.58\text{mm}$$

Further, based on the shear spinning's constant volume law wherein the volume of the participating deformation section is

equal to the volume of the corresponding finished product, we then suitably considered the machining allowance, determined the diameter to be 450mm and the dimensions of the spinning slab to be: $\phi 450 \times 2.5$.

(3) Spinning Parameter Selection and Its Spinning Results

Table 2 lists the spinning parameters and spinning results of some of the parts. We can see from the table that the clearance Z value between the rotating wheel and mandrel directly influences the degree of deviation of the sinusoidal rate and is thus related to whether or not the part can be spun to completion.

The degree of deviation of the sinusoidal rate is Δ ,

$$\Delta = \frac{(1)t_{\text{actual}} - t_{\text{theoretical}}}{t_{\text{theoretical}}} \times 100\% \quad (2)$$

(3)

Key: (1) Actual; (2)-(3) Theoretical.

In the formula:

t_{actual} is the actual thickness of the part;

$t_{\text{theoretical}}$ is the theoretical thickness of the part.

(1) 序 号	(2) 板坯及厚度 (MM)	(3) 旋 压 参 数			(7) 旋 压 结 果			
		主轴转速 (4) n	进给量 (5) f	间 隙 (6) Z				
		MM/分	MM/分	MM	(8) 旋压工作 状 态	L MM	t MM	$\frac{\alpha}{2}$
1	1Cr18Ni9Ti $t_o=2.5$	90	20	0.4 (9) 断 裂				
2	1Cr18Ni9Ti $t_o=2.5$	100	20	0.25 (10) 旋压正常	150	0.71~0.75	18°30'	
3	1Cr18Ni9Ti $t_o=2.5$	110	20	0.25 (11) 旋压正常	152	0.71~0.75	18°30'	
4	1Cr18Ni9Ti $t_o=2.5$	90	20	0.25 (12) 旋压正常	165	0.71~0.75	18°30'	
5	1Cr18Ni9Ti $t_o=2.5$	90	25	0.25 (13) 旋压正常	146	0.71~0.75	18°30'	
6	1Cr18Ni9Ti $t_o=2.5$	90	25	0.25 (14) 旋压正常	146	0.71~0.75	18°30'	
7	1Cr18Ni9Ti $t_o=2.5$	90	20	0.25 (15) 旋压正常	143	0.71~0.75	18°30'	
8	1Cr18Ni9Ti $t_o=2.5$	90	20	0.25 (16) 旋压正常	143	0.71~0.75	18°30'	
12	1Cr18Ni9Ti $t_o=2.5$	90	20	0.25 (17) 旋压正常	143	0.71~0.75	18°30'	
01	C-103 $t_o=2.6$	90	20	0.2 (18) 旋至20mm 断 裂				
02	C-103 $t_o=2.6$	90	20	0.3 (19) 旋压正常	157	0.75~0.8	18°10'	
03	C-103 $t_o=2.6$	90	20	0.3 (20) 旋压正常	157	0.8~0.85	18°10'	
04	C-103 $t_o=2.6$	90	20	0.3 (21) 旋压正常	152	0.8~0.85		
05	C-103 $t_o=2.6$	90	20	0.3 (22) 旋压正常	152	0.8~0.85	18°10'	
06	C-103 $t_o=2.6$	90	20	0.15 (23) 断 裂				
07	C-103 $t_o=2.6$	90	20	0.3 (24) 旋压正常	143	0.74~0.78	18°30'	
08	C-103 $t_o=2.6$	90	20	0.3 (25) 旋压正常	143	0.74~0.78	18°30'	

Table 2

Key: (1) Sequence number; (2) Slab and thickness;
 (3) Spinning parameter; (4) Rotating speed
 of principal axis; (5) Feed quantity;
 (6) Clearance; (7) Spinning results; (8) Oper-
 ating state of spinning; (9) Fracturing;
 (10)-(17) Spinning is normal; (18) Spinning to
 20mm, fracturing; (19)-(22) Spinning is normal;
 (23) Fracturing; (24)-(25) Spinning is normal.

If clearance Z value tends to be small, then the thickness of
 the actually spin out part t_{actual} is small. At this time,

$t_{actual} < t_{theoretical}$, Δ is a negative value which is called the "thinning excess" and the part has possible rotation damage. We should amplify the Z value for this situation and make great efforts to cause $\Delta \rightarrow 0$ and this can guarantee relatively good spinning quality.

(4) Forming of the Nozzle's Rounded Angle Arc Section

In order to resolve that the circular arc section of rounded angle R4 can maintain thickness equal to that of the conical wall, we used "the cutting unnecessary metal method," "the thinning the reverse side method" and the "extension forming method." Only the last method can effectively guarantee forming quality.

Figure 4 shows the situation when there is extension forming of the nozzle's rounded angle R4. It is a nozzle part which has gone through forward and reverse shear spinning, it is held on an extension frame and uses an oil press to lower the pressure for the nozzle's extension forming. We later cut out the unnecessary conical section and complete the required part.

In the present cold pressing technique, "extension forming" is still a new type of forming method and it has practical value in the area of cold pressing. Following the requirements of object advancements, in future practice, this new technique will be used to make up for the deficiency of cold pressing techniques.

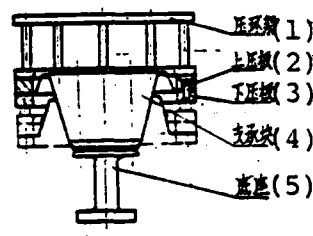


Fig. 4 Extension forming of nozzle.

Key: (1) Pressure ring frame; (2) Upper pressure plate; (3) Lower pressure plate; (4) Supporting block; (5) Base.

2. Diameter Expansion of the Nozzle

The cylindrical section and conical section of the extended nozzle are the same and it is required that they take part in the extension process simultaneously. Therefore, it is necessary to keep their wall thicknesses and conical walls uniform. When we considered simplicity and convenient conditions for existing equipment, we used the die expanded diameter method as shown in Fig. 5. When expanding the diameter, the part fixes position near the matrix conical section and makes use of the spring's pressure to cause the supporting block to firmly press on the part, the matrix to move down and the part to expand the diameter.

When the diameter of a cone is expanded and forms a cylinder, each section's degree of deformation of the deformed metal is different. In theory, the thinning quantity of the bottom of the cylinder should be largest yet in the test results the thinnest area is in the transfer area of the cylinder and conical section with about 0.06-0.08mm thinning. However, the bottom of the cylinder has about 0.105-0.06mm thinning. This is because during the diameter expansion process, the matrix is in contact with the conical wall and under the effects of friction, tensile thinning deformation occurs. Another phenomenon is after the matrix separates from the part, the cylinder section

produces localized non-circularity and this is the result of the remnant stress of the deformed metal. If we add in a supporting block then we can restore the circularity. By adding support annealing beforehand, we can eliminate local non-circularity. Annealing was not carried out during the tests.

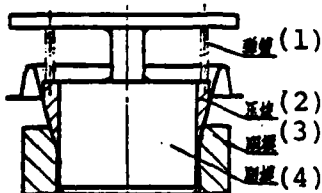


Fig. 5 Diameter expansion of the nozzle.

Key: (1) Spring; (2) Briquetting; (3)-(4) Matrix.

3. Machining

The cutting of niobium alloy requires greater cutting power than stainless steel and it is easy to have a sticky knife. The results of using a relatively small cutting amount and using a high speed cutting tool were relatively good and the cutting process could use cooling liquid.

4. Annealing During the Procedure

(1) The cold hardening of 1Cr18Ni9Ti stainless steel is very sensitive and after going through a certain amount of deformation, it is necessary to carry out thermal process softening so as to restore the plasticity of the material. The softening system which we used was: $1050 \pm 10^{\circ}\text{C}$ air quenching or water quenching, the heat preservation time was determined by the wall thickness of the part and each 1mm thickness preserved the temperature for ten minutes. The results of using water quenching softening were relatively good yet the thermal process deformation was large which was not advantageous to the later procedures. The tests proved that "air quenching" can satisfy the

requirements of forming and extension.

(2) The C-103 did not have any noticeable hardening, yet after going through relatively large deformation, it was suitable to carry out annealing which was advantageous for restoring plasticity. Annealing was carried out in a vacuum furnace with vacuity of 10^{-4} on the mercury column. The annealing temperature was $1250 \pm 5^\circ\text{C}$ and the heat preservation time was one hour.

IV. Cold Deployment Tests

In order to test and verify the design plan of the extendible nozzle and measure the extension properties of C-103 niobium alloy as well as seek related technical data and the operating process of a simulated engine nozzle, we carried out cold deployment tests on the developed extendible nozzle.

To economize on the expensive niobium alloy and reduce the procedure turnover, during the actual tests we did not machine the niobium alloy flange and thus saved on the vacuum welding and vacuum annealing procedure. After actual forming, the nozzle's R4 wall thickness was 2.5mm, the large end zone had a flanged edge and above and below we used common steel plate to hold the flanged edge so as to transmit the applied force of the cold deployment process. The cold deployment tests were carried out on an extension aiding rack located on a 450 ton oil press. Figure 6a shows the situation when the cold deployment of the conical nozzle is completed while Fig. 6b shows the situation when preparing the cold deployment of a composite nozzle.

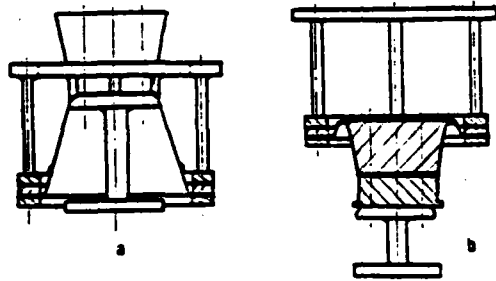


Fig. 6a

Fig. 6b

Key: a. Conical nozzle extension completed; b. Before extension of composite nozzle.

During, before and after the cold deployment tests, we used five types of nozzles to carry out tests as shown in Fig. 7. In the figure, (1) and (2) are single conical wall nozzles. During the tests, the bottom was unstable and folding occurred (see Photo 6). The (3), (4) and (5) types were carried out relatively smoothly during the cold deployment tests (see Photos 4,5).

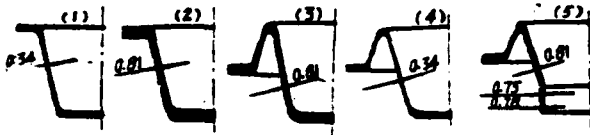


Fig. 7 Five nozzle plans taking part in the cold deployment tests.

1. Stress When There is Nozzle Extension

For plans (1) and (2) in Fig. 7, the stress during the extension process is as shown in Fig. 8(a), q is the uniform load of the hydraulic press acting on the nozzle's flanged edge and P is its resultant of forces acting on the conical wall. It

can be seen from the figure that the component of forces S value is relatively large. Moreover, the action direction is the fixed bottom, area along the conical walls pressure direction and as a result the near bottom area of the conical wall is unstable and produces folding. Component of forces S' causes the inverse conical wall to sustain tension and the tension causes the nozzle to carry out smooth extension. Because the nozzle's flanged edge stress areas are equal, therefore $P=P'$, $S=S'-P\cdot\cos18^\circ$.

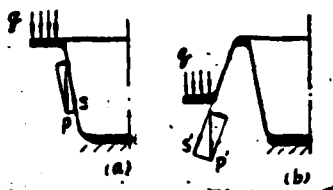


Fig. 8 Stress situation when there is nozzle extension.

During the testing process, we measured actual applied force P and we installed a pressure sensor on the bottom of the extension frame. See Fig. 9 for the measured pressure valve. We can see from the figure that the initial pressure of the nozzle extension is relatively large and this is the result of the initial extension rounded angle $R4$ being a thick wall (2.5mm). The conical section's pressure tends to be uniform and the cylinder's extension force is a bit large. Because there was no annealing after cylinder section forming, the 1Cr18Ni9Ti is very sensitive towards cold hardening and therefore the extension force in the cylinder section is higher than C-103.

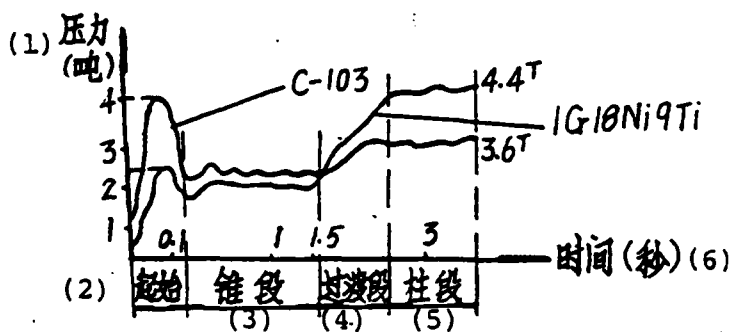


Fig. 9 Pressure-time curve of nozzle extension.

Key: (1) Pressure (tons); (2) Initial; (3) Conical section; (4) Transition section; (5) Cylinder section; (6) Time (seconds).

2. Analysis of Cold Deployment Process

Figure 10 shows the deformation of each part of the nozzle during the cold deployment process. The EF section and flanged edge part only have parallel movements during the cold deployment process and the remaining parts have point by point straight extension. All points of the metal in the extension have radial displacement. As shown in Fig. 10, point A undergoes extension and becomes point A' and its radial displacement is A'C. We will now offer the following proof.

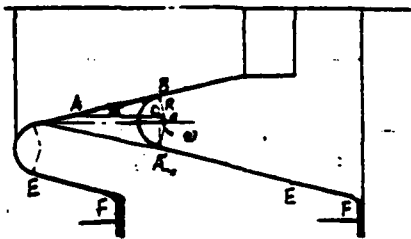


Fig. 10 Instantaneous schematic of extension process.

Hypothesis: the AB conical wall is equal to the A'B arc

length, the extension radius is R, after extension point A falls on point A' and A'C is the radial displacement of point A. We can deduce the following formulas based on Fig. 10:

$$\overline{AB} = \widehat{\overline{A'B}} = R\omega \quad (\omega \text{ 随 } \alpha \text{ 的大小而为定值}) \quad (1)$$

$$\overline{BC} = \overline{AB} \sin \alpha = R\omega \sin \alpha$$

$$\overline{CA'} = \overline{A'B} - \overline{BC} = 2R\cos\alpha - R\omega \sin\alpha$$

$$= R(2\cos\alpha - \omega \sin\alpha) \quad (2)$$

Key: (1) ω is a fixed value following the size of a.

It can be known from formula (2) that displacement CA' and extension radius R are related to the part's tapered angle. Because of the production of the radial displacement, based on the law of constant volumes it is then necessary to cause thinning or axial shortening of the part's wall thickness or both. Therefore, if the part's semi-tapered angle is already fixed, then the smaller extension radius R the better. The smaller R is the smaller the radial displacement. However, it is not advantageous for R to be too small for metallic deformation.

Figure 11 shows the strain curve of the C-103 nozzle actually measured during the extension process. The strain foils are stuck on the $\phi 332.5$ circular ring area and the strain foils are separately attached along the part's generating line and ring direction. In the figure, $\varepsilon_{\text{generating}}$ and $\varepsilon_{\text{tangent}}$ are actually measured curves and $\varepsilon_{\text{thick}}$ is a curve obtained through calculations.

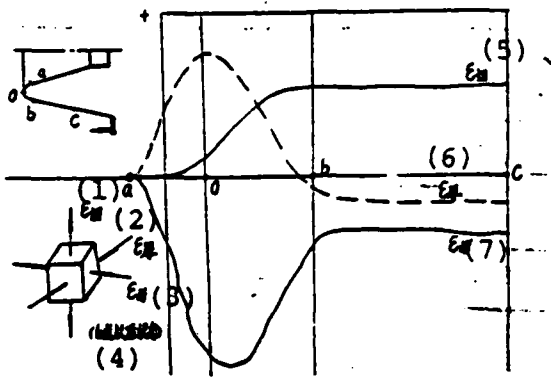


Fig. 11 Strain curves of C-103 nozzle during cold deployment process.

Key: (1) Tangent; (2) Thick; (3) Generating;
 (4) Condition of six or more points;
 (5) Tangent; (6) Thick; (7)

Because the metal's volume does not change, based on the plasticity deformation theory, there exists the following relational formula:

$$\varepsilon_{\text{tangent}} + (-\varepsilon_{\text{generating}}) + \varepsilon_{\text{thick}} = 0 \quad (3)$$

Here, $\varepsilon_{\text{thick}}$ is the curve obtained from formula (3). We should point out that in the extension process, the a-b arc section simultaneously has additional deformation of the cubic bending and thus the deformation is made even more complex. We can know from this that nozzle extension is a complex loading process, its stress-strain condition is continually changing, the maximum stress and strain strengths are located in the extension rounded angle area and the straight wall after extension basically has no strain changes. We can also see in Fig. 11 that the nozzle produces negative strain (i.e. sustains compression) along the beginning and end of generating line direction during the extension process and produces positive strain (i.e. sustains tension) along the beginning and end of the

tangential direction. The results of these two actions cause the nozzle to first gradually increase thickness during extension and when its extension is straight, it then gradually becomes thinner until it is stable at a constant thinned value. Because there are numerous influencing factors during actual measurements, here we will only make a simple quantitative analysis.

Tables 3 and 4 compare and measure the related dimensions before and after nozzle extension. We can roughly see from the tables that:

- (1) After the part undergoes extension, this can maintain or slightly raise its precision.
- (2) After extension, the conical wall is slightly thinner.
- (3) When comparing the part after extension and the corresponding section before extension, the radial expansion shrinks along the generating line.

(1) 喷嘴材料	(2) 不圆度		(5)母线不直度		(8)半锥角		(11)壁厚	
	(3)展前	(4)展后	(6)展前	(7)展后	(9)展前	(10)展后	(12)展前	(13)展后
C-103	0.7	0.24~0.3	0.05	0.05	18°14'	18°30'	0.78	0.75
1Cr18Ni9Ti	0.6	0.3	0.08	0.08	18°30'	18°30'	0.75	0.70

Table 3

Key: (1) Nozzle material; (2) Non-circularity;
 (3) Before extension; (4) After extension;
 (5) Non-linearity of generating line;
 (6) Before extension; (7) After extension;
 (8) Semi-conical angle; (9) Before extension;
 (10) After extension; (11) Wall thickness;
 (12) Before extension; (13) After extension.

(1) 零件状态	l_1 , mm	l_2 , mm	l_3 , mm	ϕ_1 , mm	ϕ_2 , mm	ϕ_3 , mm	ϕ_4 , mm	ϕ_5 , mm
铌合 (5) 展 前	29.2	58.3	15	345.7	332.5	314.5	310	300
金 (6) 展 后	28.7	57.5		358.5	341.8	324.2	321.8	310.8
不 (7) 展 前	29	53.1	15	346.5	332	313.5	313.3	300
钢 (8) 展 后		52.4		359.3			324	311
不 (9) 展 前	30.2	53.7	15.7	341.3	332.5	312.5	306.4	300
钢 (10) 展 后	29.7	52.96		354.7	342.8	325.2	319.3	312.5

Table 4

Key: (1) Part's condition; (2) Niobium alloy;
 (3)-(4) Stainless steel; (5) Before extension;
 (6) After extension; (7) Before extension;
 (8) After extension; (9) Before extension;
 (10) After extension.

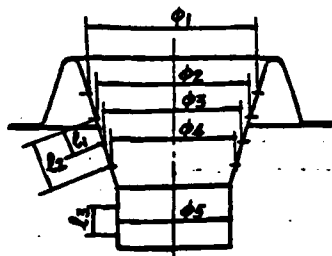


Fig. 12 Figure attached to Table 4.

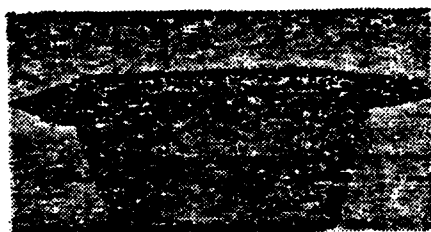
V. Conclusion

1. The forming technique of the extended nozzle's medium-sized cold test piece used the comprehensive method of shear spinning-extension-forming mandrel diameter expansion which can machine parts that accord with the test requirements and obtain excellent sectionality. If the extended nozzle's amplified dimensions undergo initial sample development, technologically, this method has continuity.

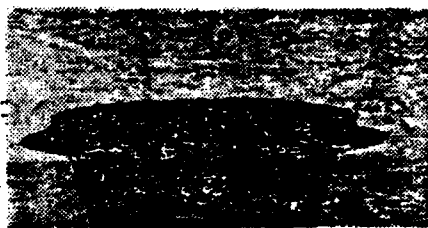
2. The initial results after cold deployment tests can be considered a basically feasible design plan for medium-sized test pieces of extended nozzles. The extension properties of C-103 niobium alloy are excellent.

3. After the nozzle undergoes cold deployment, the radial enlargement is about 3%, the generating line shortening is about 1% and the wall thickness thinning is about 3%.

VI. Appended Photos



(1)第一次强力旋压



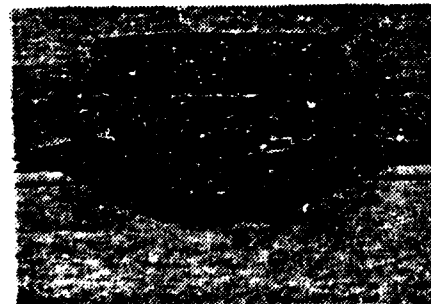
(2)第二次强力旋压



(3)切底后扩径



(4)锥形件冷展以后



(5)复合形件冷展以后



(6)单锥体冷展时失稳情况

Figs. 1-6 (continued on next page).

Figs. 1-6 (continued).

- Fig. (1) The first shear spinning.
- Fig. (2) The second shear spinning.
- Fig. (3) Enlarged radius after cutting the base.
- Fig. (4) After conical piece cold deployment.
- Fig. (5) After composite piece cold deployment.
- Fig. (6) Instability when there is single cone cold deployment.

References

- [1] Chen Shixian, Shear Spinning and Its Applications.
- [2] B. π Luomanruofusiji, Cold Pressing Technology.
- [3] Rare Metal Alloy Machining, No. 3(1979).
- [4] The Behavior of Austenitic Chromium Nickel Steel in Conjunction With Flow Turning.

END